Oligosaccharides as Model Systems for Understanding Water−Biopolymer Interaction: Hydrated Dynamics of a Hyaluronan Decamer

A. Almond,* A. Brass, and J. K. Sheehan

Division of Biochemistry, School of Biological Sciences, University of Manchester, Oxford Road, Manchester, M13 9PT, United Kingdom

Received: February 10, 2000

Hyaluronan is a mammalian extracellular maxtrix polysaccharide with unusual physiochemical properties. In this study, a five-nanosecond simulation of a hyaluronan decasaccharide in aqueous solution was compared with previous experimental data and hence used as a model system for studying carbohydrate−water interactions. The predicted average conformation is in agreement with X-ray fiber diffraction and hydrodynamic predictions, but the calculated persistence length is larger than that inferred from experiments, as is expected from the lack of counterions in this simulation. Intramolecular hydrogen bonds were observed in the simulation across all sugar linkages, but they are predicted to be in exchange with water and with themselves. Some 80 distinct intramolecular hydrogen-bond interactions were documented over a period of 1 nanosecond in this short length of polymer. Therefore, it is predicted that individual intramolecular hydrogen bonds will be difficult to observe directly by nuclear magnetic resonance spectroscopy or other experimental techniques. However, the simulation also predicts that this exchange is atypical at the terminal linkages of the polymer. Such end-effects have been proposed from interpretation of nuclear magnetic resonance spectroscopy and circular dichroism measurements. In summary, water interaction resulted in a molecular end-to-end distance that was consistently close to the maximum. However, there were strong but ephemeral fluctuations on the subnanosecond time scale away from the most extended state, involving large rearrangements of the surrounding water structure. This dynamic model for hyaluronan extends the current static microscopic view, while also being consistent with large-scale stiffened random-coil models. Therefore, it is proposed that these microscopic properties, emergent from water interaction, are responsible for the macroscopic physicochemical properties of this molecule. These results motivate the design of novel prediction-testing experiments, which can throw new light on water−biopolymer interactions.

1. Introduction

Biomolecular shape, and therefore function, is emergent from a dynamic interplay with water. However, dynamic interactions involving water are extremely complicated and difficult to imagine,[1] and therefore the relationship between the microscopic interactions of water with biomolecules and macroscopic behavior is presently unclear. This situation is restricting our understanding of important biological phenomena. We propose that computer simulations, when they can be compared effectively with experiment, can be used as a bridge between physical theory and experimental observations. This is now timely because of the widespread accessibility of fast computing facilities, which are required to model large molecular systems. Since the functions of carbohydrates are intimately related to dynamic interactions with liquid water,[2] they are excellent model systems for studying water−solute interplay. In this study, we have used the polysaccharide hyaluronan as a model system and have attempted to illuminate its dynamics in water and provide a relationship to biological function.

Hyaluronan (HA) is a linear, high molecular mass ($10^5 - 5 \times 10^6$ Da) polysaccharide composed of a simple repeating unit of *N*-acetyl-D-glucosamine and D-glucuronic acid containing alternating $\beta(1 \rightarrow 3)$ and $\beta(1 \rightarrow 4)$ linkages. It has a fundamental role in a myriad of interactions within tissue extracellular matrix, which result from its physiochemical properties.[3] The ubiquity and importance of HA as a biological polymer has made it the subject of continuous experimental study over the last thirty years. However, HA gained renewed importance as a biomaterial over the last decade.[4] The resultant industries have provided a ready supply of good-quality material, which has recently intensified the experimental study of HA. Its structure was originally solved in the solid-state by X-ray fiber diffraction in a number of cationic environments. Left-handed 4-fold helices were found in sodium and potassium environments, and left-handed 3-fold helices were found in calcium environments.[5] Under acidic conditions, an extended 2-fold helix has been observed.[6] All of these structures are consistent with the presence of intramolecular hydrogen bonds across the glycosidic linkages.[7] Many hydrodynamic measurements have been performed on HA solutions, using viscometry, ultracentrifugation,[8] visible light scattering,[9] and X-ray scattering.[10] From this data, a model for HA has been proposed in which it acts as a stiffened wormlike coil in solution.

A hypothesis invoking intramolecular hydrogen bonds was proposed to explain the apparent stiffening of the HA chain.[11] This was supported by observations of alkali-induced conformational changes in HA[12] and the anomalously low rate of its periodate oxidation kinetics.[13] In this model, the linkages are

* Corresponding author. Presently at the Department of Chemistry, Carlsberg Research Centre, Gamle Carlsberg Vej 10, Copenhagen, DK-2500, Denmark. Tel.: +45 33 27 52 03. Fax: +45 33 27 47 08. E-mail: aa@crc.dk.

10.1021/jp000402t CCC: $19.00
Published on Web 05/20/2000

restricted by intramolecular hydrogen bonds between the sugar residues. Subsequent nuclear magnetic resonance (NMR) experiments have indicated their existence in dimethyl sulfoxide,[14] but experiments proved inconclusive in aqueous solution.[15] A current three-dimensional microscopic model for HA in solution is that of a rather static, stiffened molecule, dominated by the presence of an extended two-fold helix.[16] This model has been offered to explain the proposed interaction between HA chains.[11]

Our previous calculations on solvated disaccharides and tetrasaccharides of HA predicted that intramolecular hydrogen bonds existed frequently between sugar residues,[17,18] in agreement with the currently accepted model, for HA. However, the oligosaccharides were observed to be in dynamic exchange between conformations, and consequently, the intramolecular hydrogen bonds were also in exchange. Particularly, we observed anomalous behavior at the ends of tetrasaccharides. Both NMR and circular dichroism (CD) observations of HA oligsaccharides have been interpreted in terms of end sugars and internal sugars.[19,20] However, to provide a correct indication of end-effects and polymeric behavior, simulations of longer oligosaccharides are required. The minimum size of oligosaccharide required to provide data on the polymer would be predicted to have a size on the order of the polymer persistence length. Current estimates indicate that the persistence length of HA is less than 5 nm,[21] a size comparable to that of a decasaccharide. Here, we report a 5-ns molecular dynamics simulation of a decasaccharide in aqueous solution. The simulation is compared with literature experimental data to establish the predictive capacity of such a technique. However, at the center of our philosophy is the proposal that simulations motivate the design of novel prediction-testing experiments, which will throw new light on biopolymer structure in general.

2. Results

A HA decasaccharide surrounded by 2000 water molecules was simulated for a total time period of 5 ns, and the coordinates were sampled from the simulation at 0.1-ps intervals. The conformation at each of the nine linkages can be described by a pair of angles, ϕ and ψ (see methods for definition). These angles were calculated from the simulation data and are plotted in Figure 1. Since we confirmed that all sugar residues maintained the $^4C_1$ ring conformation over the whole simulation, these plots describe the range of movement of each linkage. In this simulation, the five $\beta(1 \rightarrow 3)$ linkages explored a similar range of angles and would therefore be predicted to behave similarly in solution. Comparison between the range of exploration of $\beta(1 \rightarrow 3)$ and $\beta(1 \rightarrow 4)$ linkages indicates that $\beta(1 \rightarrow 4)$ linkages are inherently more mobile than similar $\beta(1 \rightarrow 3)$ linkages within the HA structure. However, the range of movement at $\beta(1 \rightarrow 4)$ linkages is predicted to be dependent on their position in the decasaccharide chemical structure. The two innermost $\beta(1 \rightarrow 4)$ linkages were observed to have a similar overall behavior, as were the two outermost $\beta(1 \rightarrow 4)$ linkages. This symmetry in dynamical behavior at either side of the central $\beta(1 \rightarrow 3)$ linkage is clear evidence of end-effects. Consequently, the innermost $\beta(1 \rightarrow 4)$ linkages are predicted to be the most polymer-like.

Intramolecular hydrogen-bond interactions were calculated over the first nanosecond of the simulation, and the results are presented in Figure 2. In this figure, the hydrogen-bond interactions are numbered sequentially, according to when they were first observed in the simulation. Over this first nanosecond, about 80 such interactions were observed, and the envelope becomes asymptotic to a constant value after this time. Thus,

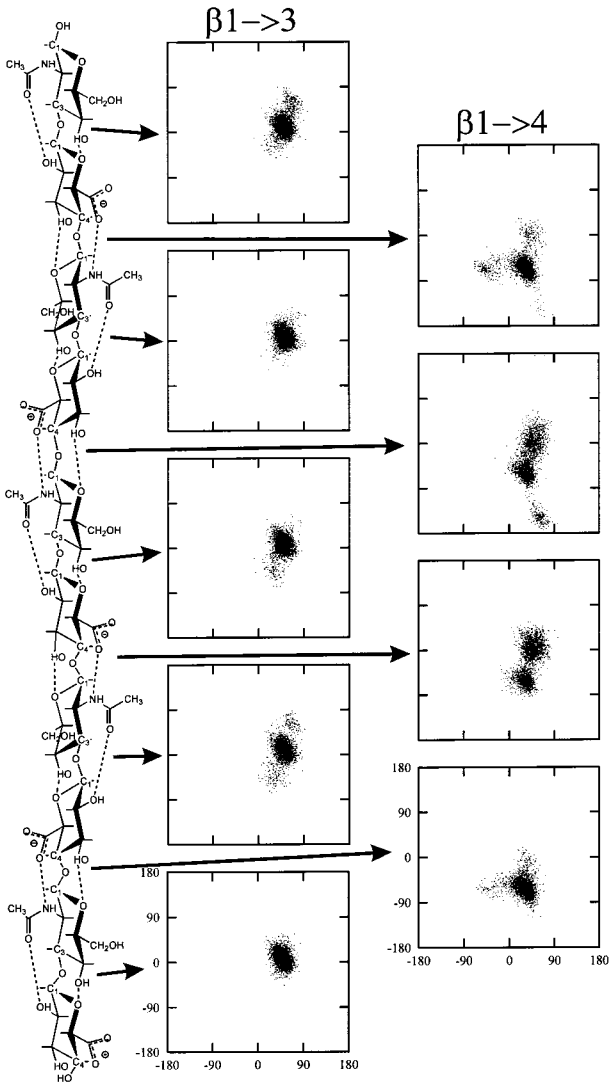

Figure 1. A schematic representation of the simulated HA decasaccharide, showing the exploration of (ϕ,ψ) angles at each of the linkages. See Materials and Methods section for the definition of the (ϕ,ψ) angles.

during the following four nanoseconds of simulation, the number of interactions did not increase substantially, suggesting that a large proportion of the local phase space was visited in this time. From this data, it is predicted that the first 200 picoseconds of simulated time is a key period over which the majority of intramolecular interactions are discovered in this molecule.

The dynamics of intramolecular hydrogen-bond exchange with water is predicted to be rapid, on the subnanosecond time scale. This is represented by Figure 3, where the total number of intramolecular hydrogen bonds have been plotted as a function of time. The total number of such interactions fluctuates rapidly, typically over periods of 10 picoseconds. Such fluctuations are consistent with the random exchange of decasaccharide with water molecules, which are diffusing into and out of the closest solvation shell. However, there are slower trends in the number of intramolecular hydrogen bonds. These fluctuations are observed over periods on the order of 200 picoseconds and correspond to long-time scale rearrangements of solute and the immediately surrounding water. Such fluctuations are intrinsically interesting since they can result in changes of molecular conformation. Each different conformation is a probable state in the HA−water ensemble. Thus, it is difficult to predict in advance which HA conformations will and will not be probable, which highlights the importance of these extensive simulations.

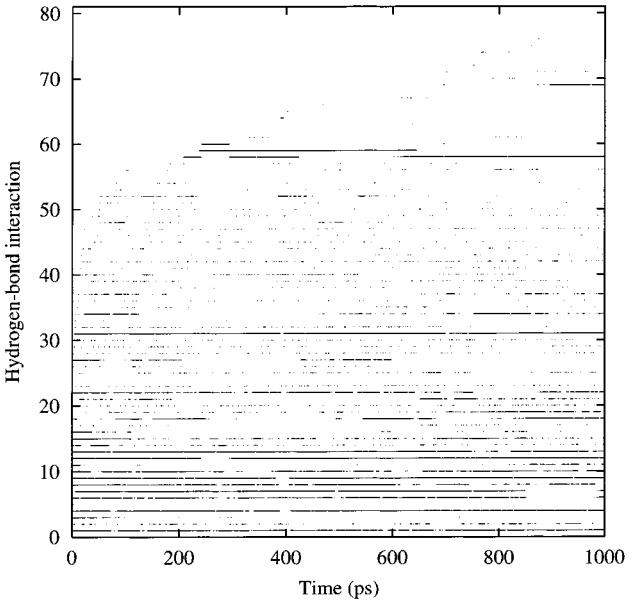

Figure 2. The occurrence of all possible intramolecular hydrogen bonds over the first nanosecond of simulation of an HA decasaccharide. They are numbered sequentially according to when they are first observed in the simulation.

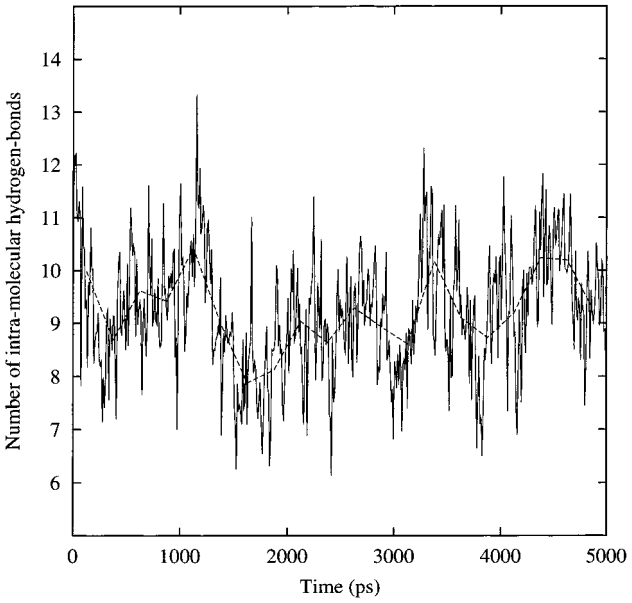

Figure 3. Total number of intramolecular hydrogen bonds observed as a function of time within a simulated HA decasaccharide in solution. The solid line is averaged over 10-ps sections, and the broken line is averaged over 250-ps sections.

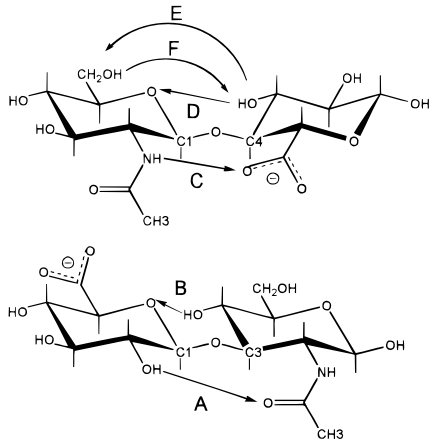

Figure 4. The major observed persistent intramolecular hydrogen bonds calculated from a simulated HA decasaccharide in solution.

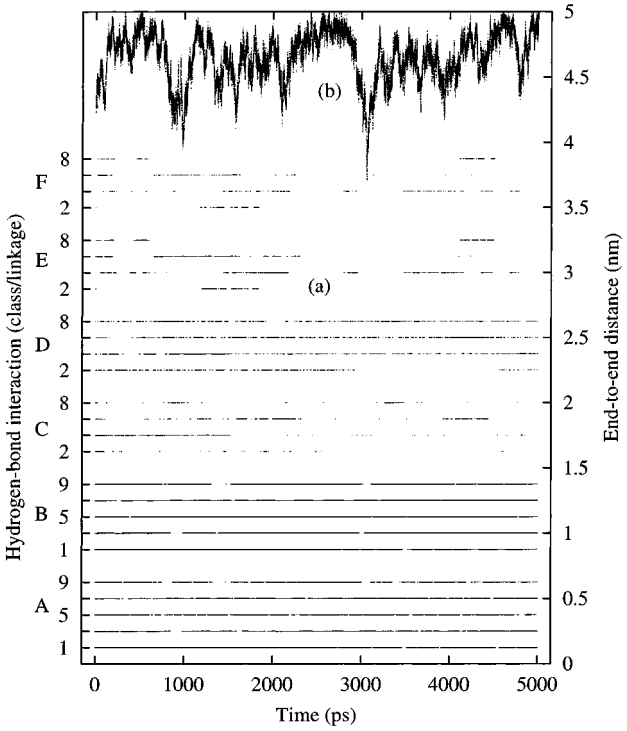

Figure 5. (a) Presence of the intramolecular hydrogen bonds described in Figure 4 at each of the linkages of a simulated HA decasaccharide in solution. Interactions at $\beta(1 \rightarrow 3)$ and $\beta(1 \rightarrow 4)$ occur at five and four possible linkages. These are plotted from the nonreducing end of the molecule. (b) The molecular end-to-end distance from the simulated HA decasaccharide in solution.

Six classes of intramolecular hydrogen-bond interactions, emergent from HA−water interplay, were deemed to be important in the dynamics of this decasaccharide, and these are labeled A−F in Figure 4. The interactions described in Figure 4 are those observed to be most persistent during the simulation. However, the arbitrary naming convention, used for interactions in Figure 2, conceals the relationship between these interactions and the dynamic behavior of the decasaccharide. Therefore, this plot was reconstructed; interactions were clustered according to the class definitions of Figure 4, and the time axis was extended to cover the whole 5 ns of the simulation. This revised plot is shown in Figure 5a. Interaction classes (A) and (B) were present at all five $\beta(1 \rightarrow 3)$ linkages, and similar interactions (C) to (F) were observed at all four $\beta(1 \rightarrow 4)$ linkages. As the *y*-axis of Figure 5a is ascended, particular linkages are identified from the nonreducing terminus of the decasaccharide, within each class of interaction. Figure 5a reveals that interaction classes (A) and (B) are particularly persistent. These interactions involve the acetamido and ring oxygens at $\beta(1 \rightarrow 3)$ linkages and are uniformly persistent along the length of the whole molecule. At $\beta(1 \rightarrow 4)$ linkages, interaction class (D) involving the ring oxygen is observed to be metastable, whereas the others, classes (C), (E) and (F), have an even lower stability than this.

The molecular end-to-end length of the decasaccharide is a useful descriptor of total molecular conformation, and its average is a macroscopically accessible property. The plot in Figure 5b shows molecular end-to-end length as a function of time for the decasaccharide. This has been aligned with the intramolecular interactions of Figure 5a, providing a relationship

TABLE 1: Angular Correlation between Disaccharide Segments, Defined by Glycosidic Oxygens at $\beta(1 \rightarrow 4)$ Linkages[a]

correlation	1	2	3	4	5
1	1.000	0.879	0.823 (10.1)	0.786 (12.2)	0.755 (13.9)
2		1.000	0.929	0.873 (14.4)	0.840 (16.9)
3			1.000	0.935	0.883 (15.8)
4				1.000	0.943
5					1.000

[a] The numbers run from the nonreducing end of the molecule. The figures in parentheses show the persistence length calculated using the respective angular correlation and the average disaccharide length (0.98 nm).

between microscopic and macroscopic behavior of the molecule. A primary observation is that the molecule is predicted to be very extended. The maximum length for this decasaccharide is approximately 5.0 nm, and during the simulation, the end-to-end length of the molecule was observed to remain close to this value. As described above, interactions around the $\beta(1 \rightarrow 3)$ linkages were observed to be persistent, and hence, it is suspected that this linkage contributes little to fluctuations in molecular length; this is in agreement with the data in Figure 1. Thus, the carbonyl oxygen and glucosamine OH2 are predicted to have a stabilizing effect on the HA solution structure. However, the observed large deviations in the $\beta(1 \rightarrow 4)$ conformation can affect molecular end-to-end length and produce the fluctuations of Figure 5b. Although all $\beta(1 \rightarrow 4)$ linkages have a dynamic behavior, those close to the center of the molecule will have the largest effects on the molecular end-to-end length. Taken together, this data suggests that water interaction at the amide proton, the carboxyl, the glucuronic acid OH3, and the glucosamine OH6 are responsible for the observed length fluctuations. The relative persistence of interaction (D) indicates a constant water environment irrespective of conformation, and thus, interactions involving the glucosamine ring oxygen are responsible for partial stabilization of the $\beta(1 \rightarrow 4)$ linkage.

Although the end-to-end length is suggestive of an extended molecule, an estimation of the persistence length was attempted to compare directly with experiment. The angular correlations between disaccharide units within the polymer were calculated, as described in the Materials and Methods section. This data is presented in Table 1, in which the vectors corresponding to all five possible disaccharides have been correlated together. The matrix of correlated values is intrinsically symmetric, and hence, only the upper triangular portion has been filled. Over the length of this decasaccharide, the angular correlation decays to 0.76. The persistence length was estimated using all correlations over more than a single disaccharide, and these values are shown in parentheses within Table 1. Thus, the persistence length of HA, in the absence of cations, is estimated from this simulation to be 13.9 ± 2.2 nm.

3. Discussion

Scott has argued for the presence of intramolecular hydrogen bonds between carboxyl and *N*-acetamido, which was initially based on the reduced rate of periodate oxidation of HA in solution.[13,22] Many of the interactions of HA and its hydrodynamic properties were later hypothesized to result from these interactions.[11,23] In this model, intramolecular hydrogen bonds involving the acetamido group are proposed to stabilize the linkage, consistent with the dramatic decrease in hydrodynamic volume of HA and the simultaneous increase in amide proton mobility associated with alkali conditions.[12] A two-fold-like

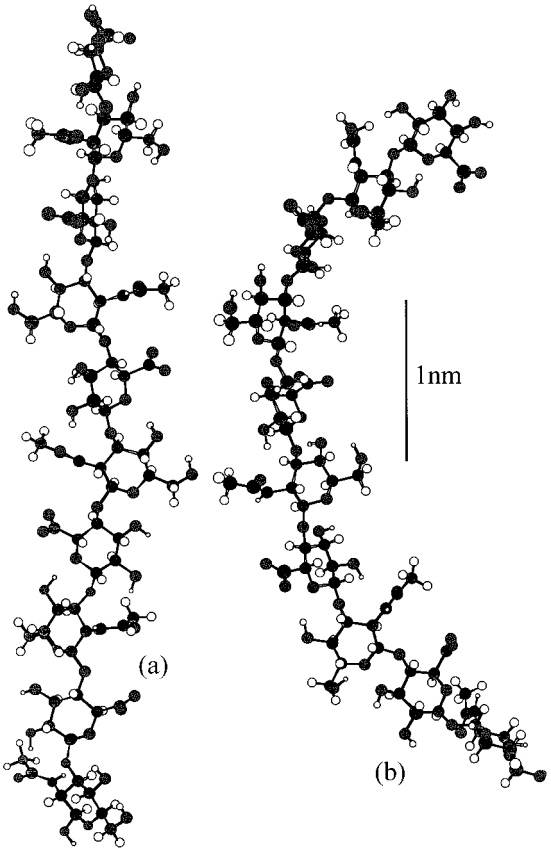

Figure 6. Two images of the simulated HA decasaccharide: (a) in an extended conformation, close to the theoretical maximum of 0.5 nm taken at time 2624.3 ps and (b) a relatively contracted conformation close to 0.37 nm taken at a time of 3060.0 ps.

conformation, associated with a fully extended HA state, has been postulated to provide the basis for HA interchain interaction.[16] This extended conformation is undoubtedly possible and is present for short periods of time in this simulation (see Figure 6a). However, the decasaccharide in this simulation was observed to have an average length of 4.5 nm and to be within 0.3 nm of this value for the majority of the simulation. X-ray fiber diffraction studies of HA with either Na^+ or Ca^{2+} cations[5,7,24] observe chains with axial rises per disaccharide of between 0.85 nm and 0.95 nm, which predicts a decasaccharide with upper and lower length limits of 4.25 nm and 4.75 nm respectively. These values fit well with the average length, and deviation, predicted from our simulation.

Contracted forms of the decasaccharide (Figure 6b), with length 4.0 nm, are intrinsically interesting and were observed in our simulation ephemerally during rapid, discontinuous changes in its trajectory. Glucuronic acid OH3 is predicted to play a key role in all these fluctuations because in the simulation they result from changes in $\beta(1 \rightarrow 4)$ conformation; it is therefore proposed that this hydroxyl is particularly important in the HA structure and perhaps at the $\beta(1 \rightarrow 4)$ linkages of other carbohydrate structures. From the observed intermittent interaction between *N*-acetamido and carboxyl, Figure 5a, it is predicted that these groupings spend a reasonable fraction of their time in a water-bridged state. In contrast, interactions involving the acetamido and ring oxygen are predicted to be more stable across $\beta(1 \rightarrow 3)$ linkages. This predicted increased mobility of the $\beta(1 \rightarrow 4)$ linkage as opposed to the $\beta(1 \rightarrow 3)$ linkage was also proposed previously on the basis of NMR and modeling data.[25] However, a recent interpretation of ^{13}C NMR spectra of HA found little difference between the mobility of

the two linkages.[26] However we would expect the presence of cations, especially calcium, to modulate the environment of the carboxyl group and its interaction with the *N*-acetamido. Thus, conclusions about the relative dynamics of the linkages must remain tentative.

The persistence length of HA has been calculated from experimental data, and values of 4−5[10] and 8 nm[9] were obtained in 0.2−0.5 M sodium chloride solution. Recent reconsideration of excluded volume effects produced more accurate values of 4.2 and 4.1 nm in 0.2 M and 0.5 M sodium chloride, respectively.[21] From this simulation, a larger value, approximately 14 nm, is predicted. However, direct comparison of persistence length between small polyelectrolytes and their polymers is only approximate as the persistence length may not be constant over all scales, although the value calculated from a simulation of HA without cations is expected to be larger than that measured experimentally. The inevitable presence of cations under experimental conditions provides electrostatic screening, thereby relaxing the molecule. Experimentally, HA chains are observed to become more rigid with decreasing ionic strengths.[8,27] To provide comparison at the correct scale, we have recently measured the diffusion coefficients of small oligosaccharides by capillary dispersion.[28] These measurements are consistent with the small oligosaccharides having a highly extended structure, in qualitative agreement with the decasaccharide simulated here and our previous simulations of tetrasaccharides.[18]

Although there is evidence for stable intramolecular hydrogen bonds in dimethyl sulfoxide,[11] no evidence for long-lived intramolecular hydrogen bonds was found in aqueous solution.[15] The simulation helps to reconcile this experimental data. Intramolecular hydrogen-bond interactions were observed, Figure 5a, but they were found to be in dynamic exchange with different sets of intramolecular hydrogen bonds and water molecules. The exchange of intramolecular hydrogen bonds is highlighted by Figure 2. Compared to the averaging time of typical NMR experiments, the processes shown in Figure 2 are extremely rapid. It can be seen (Figure 3) that the total number of intramolecular hydrogen bonds has a consistently high value, somewhere between 6 and 14 contacts. However, the persistence length calculated from the simulation is longer than that measured experimentally. It is therefore possible that in this simulation, the structure partakes in more intramolecular associations than a relaxed structure in an ionic solution would.

This decasaccharide simulation predicts the presence of end-effects, arising from atypical conformational mobility and hydration at the ends of the molecule. This is in qualitative agreement with NMR and CD observations. The spectra obtained from vacuum ultraviolet CD observations of oligosaccharides had to be interpreted in terms of linear combinations of interior sugar residues and end sugar residues.[19] Further, depending on the oligosaccharide sequence, the end residues showed either a positive or negative band close to 190 nm, suggesting qualitative differences between terminal $\beta(1 \rightarrow 3)$ and $\beta(1 \rightarrow 4)$ linkages. In NMR studies, small oligosaccharides showed two or three separate amide proton resonances corresponding to interior or end residues.[20] A similar result was obtained in dimethyl sulfoxide.[29] However, the amide proton vicinal coupling constant was measured at a high value (9 Hz) in water and a lower value in dimethyl sulfoxide (7−8 Hz). The high value in water does not support the hypothesis of a stabilized hydrogen bond between amide and carboxyl, in which the amide would have to deviate 35−40° from a trans orientation. Instead, it was proposed that water molecules participated in bridging the carboxyl and acetamido groups.[30] Our data agree with this hypothesis to some extent, because we observed all amide protons to be oscillating around the trans orientation throughout the simulation. As shown in Figure 5a, interactions between carboxyl and amide do occur, but in this simulation these groupings are predicted to interact more often with water molecules.

Simulations thus provide an alternative view of HA, in which it behaves as a stiff flexing coil that can locally undergo discontinuous changes in direction. This view of the molecule would reconcile two important observations, not only its extended nature alluded to above, but also its extreme solubility, even at high molecular weight, and its inability to make purely elastic gels[31] (rapid fluctuations in chain direction provide a basis for avoiding self-association). The presence of such high-frequency fluctuations is a direct prediction of this simulation, and use of high-frequency correlation methods could provide a sensitive experimental test of this, and similar, simulations. It would not only provide verification but also a potential means of refining molecular dynamics simulations, which is currently a desirable goal. However, at present we can offer no clear causal explanation of this predicted dynamic behavior, other than that it is an emergent property of the combined water−polymer ensemble. The simulations predict that the flexing dynamical motion of the molecule is dominated by water interaction, which stabilizes and destabilizes specific intramolecular interactions. We find the presence of these long-lived intramolecular interactions, especially those involving the *N*-acetamido group, somewhat mysterious at present. A possible explanation is that these local conformations are highly favored because they cause the least disturbance to the surrounding water organization. In the case of HA, these favorable configurations coincide with extended states, and water redistribution around these configurations generate the dynamics observed in this simulation of HA. The emergent solution conformation and dynamics of HA, we hypothesize, are sufficient to explain many of its physical properties, which are central to its biological function.

4. Conclusion

The present simulation of hyaluronan in aqueous solution shows good agreement with experimental data. The predicted end-to-end length distribution shows correspondence to the different hyaluronan fiber crystal morphologies characterized by X-ray fiber diffraction. The persistence length predicted from the simulation (14 nm) is larger than that obtained from experiments (4−8 nm). However, this was anticipated because the simulation was performed without counterions. We observed intramolecular hydrogen-bond interactions across all decasaccharide linkages. The acetamido group, a general feature of glycosaminoglycans, was involved in many of these interactions. However, we observed that all intramolecular hydrogen bonds were rapidly rearranging and exchanging with water, and a high proportion of all possible intramolecular hydrogen-bonding interactions were observed over a period as short as 200 ps. Therefore, it is predicted that although intramolecular hydrogen-bond interactions exist, they may not be persistent enough to be observed in aqueous solution from temperature changes of proton chemical shifts, as observed by nuclear magnetic resonance spectroscopy. This would explain why intramolecular hydrogen bonds are inferred to exist in dimethyl sulfoxide but not in aqueous solution.

The currently accepted microscopic model for hyaluronan in solution is a static two-fold structure that is stabilized by

intramolecular hydrogen bonds between neighboring sugar residues. Although this three-dimensional structure is represented in our simulations, we now propose a more dynamic model. The simulation predicts a hyaluronan decasaccharide that is consistently close to the maximum molecular end-to-end distance, and thus the polymer would be predicted to be locally stiffened by this. However, there were strong but ephemeral fluctuations on the subnanosecond time scale away from the most extended state involving large rearrangements of the surrounding water structure, which would introduce dynamic flexing into polymer molecules.

This simulation not only provides detailed information regarding hyaluronan, but also generic information about the carbohydrate−water interactions. It is anticipated that after other similar simulations have been performed, general hypotheses relating to carbohydrate−water systems will be devised, which will motivate the design of novel experiments to test them. A significant increase in the understanding of carbohydrate three-dimensional structure will aid the elucidation of carbohydrate biological function, which is largely unclear at present. In time, hypotheses relating to carbohydrate−water interactions will add to our knowledge of how water is concomitant with all biological interactions and thus will allow predictive theories to be developed.

5. Materials and Methods

Molecular dynamics was performed with the explicit inclusion of water molecules into the simulation using the tinker program as a basis[32,33] and using AMBER-95 parameters with extensions for carbohydrates.[34,35] Partial charges were calculated with Gaussian 98,[36] using the HF/6-31G* basis set for GlcNAc and HF/6-31G** for GlcA.

Molecular dynamics integration was carried out using the leap-frog formulation[37] of the Verlet algorithm,[38] and hydrogen covalent bond lengths were kept constant using the SHAKE procedure.[39] An integration step size of 1 fs was used to provide precise trajectories. No explicit hydrogen-bonding function was used in the simulations, as it is assumed that they are well represented by the partial atom charges and van der Waals parameters.[40]

Solvated simulation employed a 6.4 nm × 3.2 nm × 3.2 nm rectangular water box filled with 2000 previously equilibrated TIP3P water molecules.[41] The initial configuration was achieved by minimization using the adopted basis Newton-Raphson approach, heating for 3 ps at a rate of 100 K ps^{-1} followed by 100 ps of diabatic equilibration at 300 K. Subsequently, 5 ns of constant-temperature dynamics (300 K) was performed by weak coupling to a heat bath to construct a canonical (NVT) ensemble. Coordinates were written every 0.1 ps, and the nonbonded lists were updated at every step. Long-range electrostatics were treated with the method of Ewald summation with a cut-off of 1.2 nm.

Glycosidic linkage conformation was represented by dihedral angles ϕ (H1−C1−O*x*−C*x*) and ψ (C1−O*x*−C*x*−H*x*) defined by the hydrogen atoms. Intramolecular hydrogen-bond interactions were calculated as in our previous work.[17,18] Our (arbitrary) definition of a hydrogen bond is identical to that used by other authors who have analyzed carbohydrate simulations.[40] A hydrogen bond is said to exist when the distance of D (hydrogen donor) to A (hydrogen acceptor) is less than 0.35 nm, and the angle D−A ... A is less than 60°. All intramolecular hydrogen bonds were identified during the simulation and characterized.

Angular correlations in the chain were calculated from vectors between disaccharide sections defined between the glycosidic oxygen atoms at $\beta(1 \rightarrow 4)$ linkages. The cosine of the angle (Ω) between units with vectors $\mathbf{x_1}$ and $\mathbf{x_2}$ is related by a scalar product of their unitary direction vectors. The value calculated for $\langle\cos(\Omega)\rangle$ from the simulation is related to the persistence length (L_P) by eq 1. In this expression, S is the length between the correlated molecular segments, calculated from the average length of an HA disaccharide, 0.98 nm.

$$\langle\cos(\Omega)\rangle = \exp\left\{-\frac{S}{L_P}\right\} \tag{1}$$

Acknowledgment. This work was supported by a fellowship provided by the Wellcome Trust, grant reference number 052055.

Abbreviations

CD, circular dichroism; HA, hyaluronan; NMR, nuclear magnetic resonance.

References and Notes

(1) Franks, F. *Water Science Reviews*; Cambridge University Press: Cambridge, 1990; Vol. 5.
(2) Kawai, H.; Sakurai, M.; Inoue, Y.; Chujo, R.; Kobayashi, S. *Cryobiology* **1992**, *5*, 599−606.
(3) Fraser, J. R. E.; Laurent, T. C. *Molecular Components and Interactions*; Comper, W. D., Ed.; *Extracellular Matrix, Vol. 2*; Overseas Publishers Association: Amsterdam, 1996; pp 141−199.
(4) van Brunt, J. *Biotechnology* **1986**, *4*, 780−782.
(5) Sheehan, J. K.; Atkins, E. D. T. *Int. J. Biol. Macromol*. **1983**, *5*, 215−221.
(6) Atkins, E. D. T.; Phelps, C. F.; Sheehan, J. K. *Biochem. J*. **1972**, *128*, 1255−1263.
(7) Winter, W. T.; Smith, P. J. C.; Arnott, S. *J. Mol. Biol*. **1975**, *99*, 219−235.
(8) Cleland, R. L. *Biopolymers* **1984**, *23*, 647−666.
(9) Fouissac, E.; Milas, M.; Rinaudo, M.; Borsali, R. *Macromolecules* **1992**, *25*, 5613−5617.
(10) Cleland, R. L. *Arch. Biochem. Biophys*. **1977**, *180*, 57−68.
(11) Scott, J. E. *The Biology of Hyaluronan*; Laurent, T. C., Ed.; Ciba Foundation Symposium 143: Chichester, U.K. 1989; pp 6−20.
(12) Welti, D.; Rees, D. A.; Welsh, E. J. *Eur. J. Biochem*. **1979**, *94*, 505−514.
(13) Scott, J. E.; Tigwell, M. J. *Biochem. J*. **1978**, *173*, 103−114.
(14) Scott, J. E.; Heatley, F.; Hull, W. E. *Biochem. J*. **1984**, *220*, 197−205.
(15) Sicinska, W.; Adams, B.; Lerner, L. E. *Carbohydr. Res*. **1993**, *242*, 29− 51.
(16) Atkins, E. D. T.; Meader, D.; Scott, J. E. *Int. J. Biol. Macromol*. **1980**, *2*, 318−319.
(17) Almond, A.; Sheehan, J. K.; Brass, A. *Glycobiology* **1997**, *7*, 597−694.
(18) Almond, A.; Brass, A.; Sheehan, J. K. *Glycobiology* **1998**, *8*, 973−980.
(19) Cowman, M. K.; Bush, C. A.; Balazs, E. A. *Biopolymers* **1983**, *22*, 1319−1334.
(20) Cowman, M. K.; Cozart, D.; Nakanishi, K.; Balazs, E. A. *Arch. Biochem. Biophys*. **1984**, *230*, 203−212.
(21) Hayashi, K.; Tsutsumi, K.; Nakajima, F.; Norisuye, T.; Teramoto, A. *Macromolecules* **1995**, *28*, 3824−3830.
(22) Scott, J. E.; Tigwell, M. J. *Biochem. Soc. Trans*. **1975**, *3*, 662−664.
(23) Scott, J. E.; Heatley, F. *Biochem. J*. **1982**, *207*, 139−144.
(24) Mitra, A. K.; Arnott, S.; Sheehan, J. K. *J. Mol. Biol*. **1983**, *169*, 813−827.
(25) Holmbeck, S. M. A.; Petillo, P. A.; Lerner, L. E. *Biochemistry* **1994**, *33*, 14246−14255.
(26) Cowman, M. K.; Hittner, D. M.; Feder-Davis, J. *Macromolecules* **1996**, *29*, 2894−2902.
(27) Ghosh, S.; Xiao, L.; Reed, C. E.; Reed, W. F. *Biopolymers* **1990**, *30*, 1101−1112.
(28) Almond, A.; Brass, A.; Sheehan, J. K. *J. Mol. Biol*. **1998**, *284*, 1425−1437.
(29) Scott, J. E.; Heatley, F.; Moorcroft, D.; Olavesen, H. *Biochem. J*. **1981**, *199*, 829−832.
(30) Heatley, F.; Scott, J. E. *Biochem. J*. **1988**, *254*, 489−493.
(31)) Gibbs, D. A.; Merrill, E. W.; Smith, K. A. *Biopolymers* **1968**, *6*, 777−791.

(32) Dudek, M. J.; Ponder, J. W. *J. Comput. Chem*. **1995**, *16*, 791−816.

(33) Ponder, J. W.; Richards, F. M. *J. Comput. Chem*. **1987**, *8*, 1016−1024.

(34) Homans, S. W. *Biochemistry* **1990**, *29*, 9110−9118.

(35) Woods, R. J.; Dwek, R. A.; Edge, C. J.; Fraser-Reid, B. *J. Phys. Chem*. **1995**, *99*, 3832−3846.

(36) Frisch, M. J.; Trucks, G. W.; Schlegel, H. B.; Scuseria, G. E.; Robb, M. A.; Cheeseman, J. R.; Zakrzewski, V. G.; Montgomery, J. A.; Stratmann, R. E.; Burant, J. C.; Dapprich, S.; Millam, J. M.; Daniels, A. D.; Kudin, K. N.; Strain, M. C.; Farkas, O.; Tomasi, J.; Barone, V.; Cossi, M.; Cammi, R.; Mennucci, B.; Pomelli, C.; Adamo, C.; Clifford, S.; Ochterski, J.; Petersson, G. A.; Ayala, P. Y.; Cui, Q.; Morokuma, K.; Malick, D. K.; Rabuck, A. D.; Raghavachari, K.; Foresman, J. B.; Cioslowski, J.; Ortiz, J. V.; Stefanov, B. B.; Liu, G.; Liashenko, A.; Piskorz, P.; Komaromi, I.; Gomperts, R.; Martin, R. L.; Fox, D. J.; Keith, T.; Al-Laham, M. A.; Peng, C. Y.; Nanayakkara, A.; Gonzalez, C.; Challacombe, M.; Gill, P. M. W.; Johnson, B. G.; Chen, W.; Wong, M. W.; Andres, J. L.; Head-Gordon, M.; Replogle, E. S.; Pople, J. A. Gaussian 98, Revision A.2; Gaussian, Inc.: Pittsburgh PA, 1998.

(37) Hockney, R. W. *Methods Comp. Phys*. **1970**, *9*, 135−211.

(38) Verlet, L. *Phys. Rev*. **1967**, *159*, 98−103.

(39) van Gunsteren, W. F.; Berendsen, H. J. C. *Mol. Phys*. **1977**, *34*, 1311−1327.

(40) Brady, J. W.; Schmidt, R. K. *J. Phys. Chem*. **1993**, *97*, 958−966.

(41) Jorgensen, W. L.; Chandrasekhar, J.; Madura, J. D.; Impey, R. W.; Klein, M. L. *J. Chem. Phys*. **1983**, *79*, 926.